

High Accuracy Momentum Compaction Measurement for the APS Storage Ring with Undulator Radiation

Bingxin Yang, Michael Borland, and Louis Emery

*Advanced Photon Source, Argonne National Laboratory,
9700 South Cass Avenue, Argonne, IL 60565*

Abstract. We developed a new technique to measure the electron beam energy centroid and spread. It takes advantage of a sharp feature in the Advanced Photon Source (APS) diagnostics undulator spectrum, the drop-off in the angle-integrated flux near its fundamental photon energy. The measurement technique has a high resolution and is nearly independent of the storage ring lattice functions. In this work, we present the results of electron beam energy measurements as a function of rf frequency and obtain the momentum compaction factor of the APS storage ring to be $2.27 \pm 0.03 \times 10^{-4}$, in good agreement with theoretical value of 2.285×10^{-4} . We will also discuss methods to further reduce experimental errors, making the technique potentially the most accurate one for measuring momentum compaction factors of a storage ring.

INTRODUCTION

Noninvasive measurement of the beam energy distribution is one of the basic requirements for studying longitudinal beam dynamics in electron storage rings. In these measurements, the momentum compaction factor α_c is an important conversion factor, which links the change of the electron momentum to the change of path length (L), revolution time (τ), or rf frequency (f), [1]

$$\frac{\Delta p}{p} = \alpha_c^{-1} \frac{\Delta L}{L_0} = - \left(\frac{1}{\gamma^2} - \alpha_c \right)^{-1} \frac{\Delta \tau}{\tau_0} = \left(\frac{1}{\gamma^2} - \alpha_c \right)^{-1} \frac{\Delta f}{f_0}. \quad (1)$$

For a high-energy ring, such as the 7 GeV APS-SR, $\gamma^2 \sim 10^8$, the quantity in the parenthesis (momentum compaction) is interchangeable with α_c up to a sign change.

When longitudinal wake fields are ignored, the bunch length can be written as

$$\sigma_l \propto \sqrt{\alpha_c}. \quad (2)$$

A storage ring with very low momentum compaction factor (a quasi-isochronous ring [2]) may produce very short bunches or very high peak current or luminosity. Due to their potential application to high-energy physics and free-electron laser sources, such rings are under intense study.

The accurate experimental measurement of the momentum compaction factor, however, has been difficult to obtain, due partly to the fact that most energy-sensitive measurement techniques depend on the lattice parameters. In 1996, Tarazona et al. [3] used the on-axis third harmonic undulator radiation spectrum to derive absolute electron beam energy and energy spread, by fitting the experimental spectrum to a straightforward theoretical model. There the dispersion function at the source was no longer required, but a good knowledge of the beam sizes and divergences was still needed.

In this work, we propose and demonstrate a new measurement technique using the undulator radiation, by employing a different part of the undulator spectrum (measuring the angle-integrated spectrum near odd harmonics), and a different procedure for data treatment (comparing the derivative of the spectrum with the model calculation). The analysis and experimental data will show that this technique has the potential to become the most accurate one for measuring the momentum compaction factor in a storage ring.

BASIC TECHNIQUE

The angle-integrated undulator radiation of a single electron has been treated previously [4-6]. The spectrum is characterized by many peaks below undulator harmonic energies and sharp declines at these energies (Fig. 1). Hence the scaled derivative of the spectrum, defined as

$$D^{(0)}(\gamma, \omega) \equiv -\omega \frac{dF^{(0)}}{d\omega}, \quad (3)$$

shows sharp peaks at these harmonics. Here γ is the gamma factor of the electron, and ω is the photon energy. Figure 1 shows the angle-integrated flux spectrum of the APS undulator A calculated with XOP [7]. The scaled derivative of the spectrum was also calculated numerically. The most pronounced features of the derivative spectrum are the sharp peaks. While sharp peaks are centered on odd harmonic energies, many

broad peaks are located below all even harmonics. Further studies of the details of the derivative spectrum show that, while the derivative peak at the fundamental energy ($n = 1$) is fairly symmetric, the peaks at higher odd harmonics are increasingly asymmetric, as can be seen from the undershoots on the low-energy side of the peaks in Figure 1.

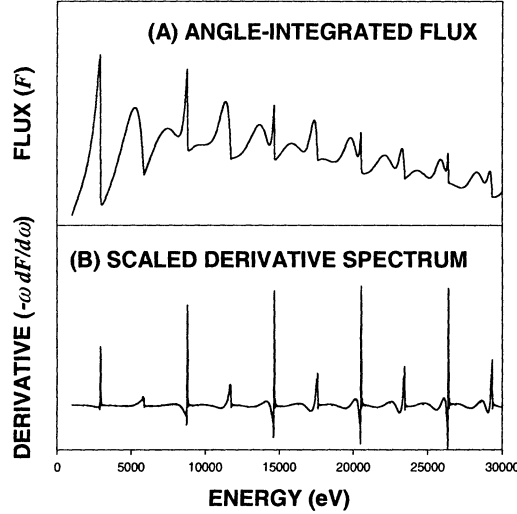


FIGURE 1. (A) The angle-integrated x-ray beam intensity of the APS undulator A. (B) The scaled derivative spectrum as defined by Eq. (3) and evaluated numerically from the total flux spectrum.

It can be shown (unpublished) that the scaled derivative has the following form,

$$D^{(0)}(\gamma, \nu) = \sin^2 \frac{\nu\pi}{2} H^{(0)}(\gamma, \nu) S_N(\nu) + C^{(0)}(\gamma, \nu), \quad (4)$$

where $H^{(0)}$ and $C^{(0)}$ are smooth functions of the electron energy γ and the dimensionless photon energy,

$$\nu = \frac{\omega}{\omega_1(\gamma, 0)}. \quad (5)$$

The function

$$S_N(\nu) = \left[\frac{\sin N\nu\pi}{N \sin \nu\pi} \right]^2, \quad (6)$$

has pronounced peaks for all harmonics ($\nu = \text{integer}$). For a large number of undulator periods, N , this function behaves very similarly to the familiar SINC function near the harmonics, $\nu \sim n$ (integer),

$$S_N(\nu) \cong \left[\frac{\sin N(\nu - n)\pi}{N(\nu - n)\pi} \right]^2. \quad (7)$$

For the fundamental photon energy ($n = 1$), the function $C^{(0)}$ is small for a large number of undulator periods, so that Eq. (2) can be simplified to

$$D^{(0)}(\gamma, \nu) \cong A \left[\frac{\sin N\delta_\omega\pi}{N\delta_\omega\pi} \right]^2, \quad (8)$$

where

$$\delta_\omega = \frac{\nu - n}{n}, \quad (9)$$

is the photon energy deviation from the fundamental resonance.

Figure 2 shows the numerically calculated derivative spectra for the APS diagnostics undulator [6] at different gap values. The SINC approximation of the function is very good over the narrow spectral region plotted except on the low-energy side, where the difference is less than 4% of the peak height.

For electron beams with finite energy spread, it can be shown that the scaled derivative spectrum of the angle-integrated undulator radiation is a convolution of the electron energy profile with the single-electron derivative spectrum,

$$D(\gamma_0, \nu_0) = \int_{-\infty}^{\infty} D^{(0)}[\gamma_0, n(1 + \delta_\omega - 2\delta)] \rho(\delta) d\delta. \quad (10)$$

One should note that the scaling of the photons energy deviation (δ_ω) and that of the electron energy deviation (δ) differ by a factor of 2 since the undulator photon energy is proportional to the square of the electron energy.

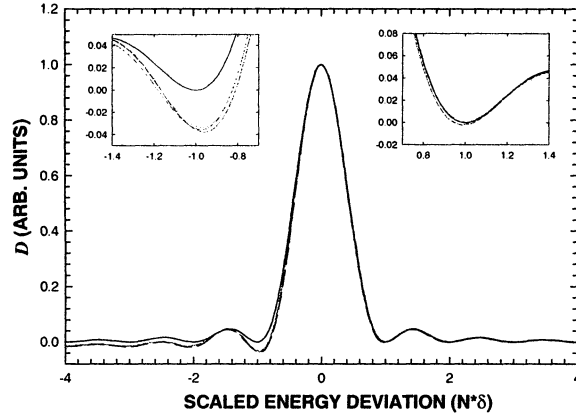


FIGURE 2. The scaled derivative spectra for the APS diagnostics undulator ($N = 198$). All spectra were normalized so that their maximum value is one. The dotted line is for $K = 0.01$, the dashed line for $K = 0.1$, the dash-dot line for $K = 0.5$, and the long-dashed line for $K = 1.0$. The solid line (top) is the SINC function.

EXPERIMENTAL SETUP

The initial experiment was performed at the diagnostics undulator beamlines of the APS [8]. Figure 3 shows the schematics of the experimental setup for measuring the angle-integrated flux. A Huber 430 goniometer was used for rotating the silicon monochromator crystal, and a 440 goniometer was used to position the monochromatic beam flux detector (a YAG scintillation detector) at 2θ . The Laue geometry was used to minimize the power absorption by the crystal. Table 1 shows other relevant parameters of the experiment. Bragg's law of crystal diffraction gives the x-ray wavelength:

$$\lambda = 2d \sin \theta. \quad (11)$$

Hence the relative photon energy change is given by

$$\frac{\Delta\omega}{\omega} = -\frac{\Delta\lambda}{\lambda} = -\frac{\Delta\theta}{\tan \theta}. \quad (12)$$

It can be converted to the equivalent electron energy deviation

$$\frac{\Delta p}{p_0} = \frac{\Delta\omega}{2\omega} = -\frac{\Delta\theta}{2 \tan \theta}. \quad (13)$$

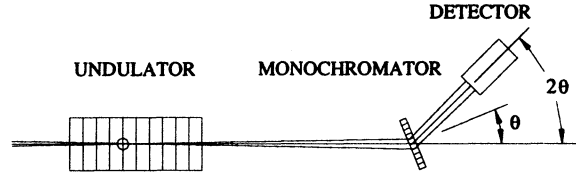


FIGURE 3. Schematic of the spectrum measurement of angle-integrated flux. The monochromator crystal uses Laue reflection with a Bragg angle θ , and the detector is located on a second rotary stage following 2θ .

TABLE 1. Relevant Parameters of the Spectrum Measurement.

Variable	Quantity
Number of undulator periods, N	198
Undulator periods, λ_u	18.0 mm
Gap, G	28.0 mm
Effective peak field	0.0129 T
Undulator parameter K	0.0217
Fundamental photon energy	25.855 keV
Monochromator crystal	Si (220)
$2d$ -spacing	0.3840 nm
Bragg angle	7.173°

Figure 4 shows a measured derivative spectrum. It is obtained by applying Eq. (3) numerically to the experimentally measured flux spectrum, obtained in a θ - 2θ scan of the monochromator. By fitting the measured derivative spectrum with Eq. (10), one obtains the centroid of the peak and the energy spread of the electron beam.

To measure the momentum compaction factor, we scanned the rf frequency of the cavity from -800 Hz to +800 Hz (central frequency = 352 MHz), at 200 Hz intervals. At each point, a θ - 2θ scan was performed to measure the derivative spectrum. The centroid energies (deviation) are plotted in Figure 5 against the rf frequency. The data points can be fitted well to a straight line. Combining Equations (1) and (13), we have

$$\alpha_c = -\frac{\Delta f}{f_0} \frac{\Delta p}{p_0} = -2 \frac{\Delta f}{f_0} \frac{\Delta \omega}{\omega_0} = -\frac{2 \tan \theta_0}{f_0} \frac{\Delta f}{\Delta \theta}. \quad (14)$$

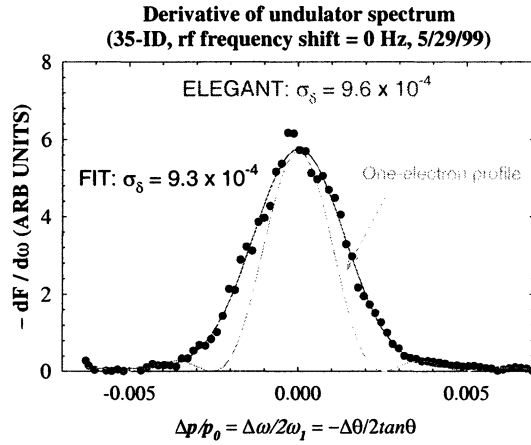


FIGURE 4. Scaled derivative spectrum of the total flux: (Dashed line) One electron radiation profile; (Circles) experimental measurements; and (Solid line) calculated value with electron energy spread assumed to be 0.93×10^{-3} .

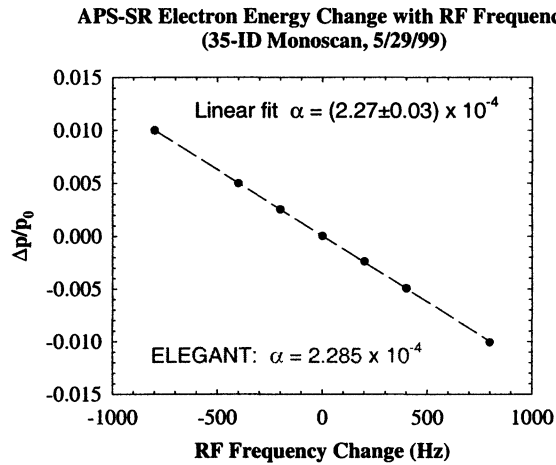


FIGURE 5. Energy centroid change as a function of rf frequency change. The slope of this curve gives the momentum compaction of the APS storage ring, 2.27×10^{-4} , compared with the simulation result of 2.285×10^{-4} .

ERROR ANALYSIS

The scaled derivative spectrum is affected by instrument factors: e-beam divergence (but not the size), undulator field error (trajectory and phase), crystal distortion and angle error (relative and offset), and rf frequency uncertainty, etc. Only

two of them have an effect on the *peak centroid* shift as a function of e-beam energy. We estimate that during the short scan time of the experiment (~ 4 hours), the rf source has maintained better than 4 Hz stability within a sweep range of ± 800 Hz, hence the error is $(\Delta\alpha_C/\alpha_C)_{\Delta f} \sim 0.25\%$. With the high-resolution Huber rotary table, the angle of rotation maintained 0.001° (4 arc-seconds) accuracy and over a small angle centroid change of $\pm 0.14^\circ$, hence the error is $(\Delta\alpha_C/\alpha_C)_{\Delta\theta} \sim 0.35\%$. From Figure 4, the statistical error of the detector is also noticeable. To estimate the effect, we use the statistical error assigned by the fit program (Fig. 5), which reflects the deviation of data point from the straight line. We estimate that the total error of the measurement is given by

$$\left(\frac{\Delta\alpha_C}{\alpha_C} \right)_{TOTAL} \sim 1\%. \quad (15)$$

CONCLUSION

We developed a new technique for extracting e-beam energy information from undulator spectrum: energy spread, energy centroid, and momentum compaction. The new technique is not sensitive to the beam size and divergence. Its accuracy depends only on precision measurements of the monochromator angle and rf frequency.

ACKNOWLEDGMENTS

This work is supported by the U.S. Department of Energy, Office of Basic Sciences, under Contract No. W-31-109-ENG-38. We would like to thank Dr. Kwang-Je Kim for helpful discussions, Frank Lenkszus for programming support, and J. Galayda and G. Decker for their encouragement and support of this project.

REFERENCES

1. Wiedmann H., *Particle Accelerator Physics I*, Springer, New York, 1993, or other standard accelerator physics text.
2. Pellegrini C., Robin D., *Nucl. Instr. Meth. A* **301**, 27 (1991).
3. Tarazona, E., Elleaume, P., et al., "Measurement of the absolute energy and energy spread of the ESRF electron beam using undulator radiation", SRI-95, *Rev. Sci. Instrum.* **67** (9) 1 (1996).
4. Krinsky, S., *IEEE Trans Nucl. Science* **NS-30**, 3078 (1983).
5. Hofmann, A., *SSRL ACD-Note* 38, 1986.
6. Kim, K.-J., "Characteristics of Synchrotron Radiation," AIP Conf. Proc. 184, 565-632 (1987).
7. Sanchez del Rio, M., and Dejus, R. J., "XOP: Recent Developments", SPIE 2448, 1998.
8. Yang, B. X., and Lumpkin, A., "The Planned Photon Diagnostics Beamlines at the Advanced Photon Source," *BIW 94, AIP Conf. Proc.* **333**, 252-258 (1995).